

Fracture Assessments of Welded Structures

T.L. Panontin, O. Nishioka
NASA Ames Research Center
Moffett Field, CA 94035

Michael R. Hill
University of California
Davis, CA 95616

Summary

Weldments are particularly susceptible to fracture due to defects, material property variations, and residual stresses created during the welding process. It is common in fracture assessments of welded structures to ignore these features; defects are often idealized to be crack-like, weld properties to be homogeneous, and residual stresses to be uniaxial and tensile or nonexistent. This paper presents an overview of several recent studies that examined the ability to accurately model fracture in welds that possess realistic flaws, inhomogeneous material properties, and residual stresses.

Introduction

Welding is a process used to permanently join two, usually metallic, components by the localized coalescence that occurs under certain combinations of temperature, pressure, and metallurgy. The range of pressure and temperature used is quite broad, although heating and cooling are integral parts of most welding processes. The particular combination of these variables results in a unique joint in terms of material variations, potential flaws, and residual stresses.

Material variations occur across a weld joint because each position in the weld is subjected to a different thermal history, with some temperatures rising above those required for phase transformations and grain growth. In a typical multi-pass weld in steel, for instance, several subzones may develop in the heat affected zone (HAZ) between the weld metal and base metal [1], each with its own microstructure and mechanical and fracture properties. Further, if filler metals are used, the weld metal may have significantly different composition than the base metal and hence may possess different mechanical properties. Such variations can cause deformation to be concentrated in the joint, as in the case of weld metals with lower strength than the base plate (undermatched), or to be forced in to the surrounding plate as occurs in overmatched welds [2]. Hence, material variations can affect both the fracture toughness and the concentration of driving force within a joint.

The welding process also largely controls the potential for weld defects to develop during fabrication. For example, the most common defects developed during arc-welding are process-related, and they include lack of penetration (LOP) and lack of fusion (LOF), which are planar or crack-like defects, and slag inclusions and porosity, which are volumetric defects [1]. Cracks may also develop during welding. Planar defects and cracks have direct consequences on the structural integrity of weldments, while volumetric defects may eventually pose problems by initiating fatigue cracks during service.

Residual stresses are created during welding by the solidification, phase transformation, and thermal shrinkage strains associated with molten weld metal as it cools. Existing without external loading, residual stresses are self equilibrating, and often reach magnitudes of yield level. They can cause cracking and distortion in weld joints and even premature failure of structures under certain conditions [1].

These factors, separately and in combination, increase the susceptibility of weldments to fracture. They also greatly complicate the application of fracture assessment methods to welded structures. Prediction of fracture is often performed by assuming that a single, global fracture parameter, such as the J -integral,

completely characterizes the conditions for fracture. However, in welds, the conditions for fracture may be affected by both residual stresses and inhomogeneous materials. Although in the former case superposition can sometimes be used to account for the driving force due to both applied and residual stresses, this requires that existing residual stresses be well characterized. In the case of mismatch where concentration of deformation is dependent on the joint materials, formulas used to estimate J for structural loadings may be inaccurate, particularly when crack sizes are small relative to the thickness of the joint [2]. Single parameter fracture methods also ignore the influence of *constraint* which affects the magnitude of the crack-tip stress fields. Two bodies loaded to the same value of the global fracture parameter, but under differing levels of constraint, will contain different levels of the crack-tip stresses and strains that ultimately set the conditions required for fracture. It has been shown that different levels of constraint can exist in structures due to differences in geometry (e.g., shallow vs. deep notch) or applied loading (e.g, tension vs. bending). Less understood is that constraint changes can also result from the presence of residual stress [3] and weld mismatch [2].

This paper presents an overview of several studies performed to examine the applicability of fracture assessment techniques to weld fracture. In the first study, the fracture behavior of an overmatched butt weld containing a buried, lack-of-penetration defect was predicted and verified experimentally. The second study examined computationally the effect of residual stresses on constraint conditions and subsequent fracture in a cracked weld. In both studies, micromechanical models were used to identify the local conditions at fracture initiation (and subsequent ductile tearing) using crack tip stresses and strains. Finite element analyses were used to predict the influence of specimen/ flaw geometry, loading mode, material flow properties, and residual stresses on the crack tip fields. Constraint effects are thus implicitly included; the critical value of the *global* fracture parameter for a particular defective weld is said to be reached when the *local* conditions for fracture are satisfied.

Realistic Flaw Geometries and Weld Material Mismatch

To assess the transferability of R-curves measured in laboratory specimens to defective structural welds, Nishioka and Panontin [4] studied the fracture behavior of an overmatched butt weld containing a simulated, buried lack-of-penetration defect. A specimen designed to simulate pressure vessel butt welds was considered; namely, a center crack panel specimen, of 1.25 in (31.8 mm) by 1.25 in (31.8 mm) cross section, loaded in tension, as shown in Fig. 1a. Specimens were loaded monotonically while load-CMOD measurements were made, then stopped and heat tinted to mark the extent of ductile crack growth. These measurements were compared to predictions made using the fracture mechanics finite element code WARP3D, which implements the Gurson-Tvergaard micromechanical model of void growth to predict ductile tearing.

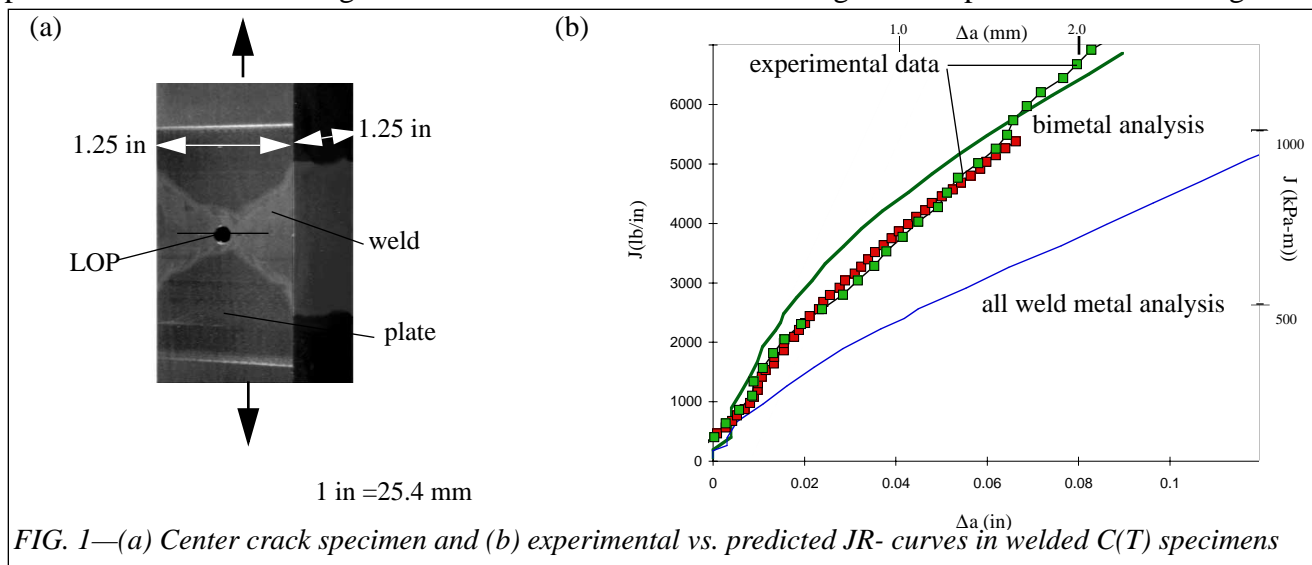


FIG. 1—(a) Center crack specimen and (b) experimental vs. predicted JR-curves in welded C(T) specimens

The stress-relieved, double-V weld tested was comprised of E7018 filler and A516-70 plate, such that the weld had a yield strength 50% higher than that of the plate material. To simulate a lack of penetration defect in the structural weld specimen, a 1/8 inch (3.2 mm) hole was drilled down the center of the weld through which a 0.003 inch (0.076 mm) diameter EDM wire was threaded. The wire was used to introduce crack-like notches toward both surfaces of the weld (Fig. 1a). Welded compact tension specimens were also tested and analyzed to provide model parameters that could not be measured directly. The R-curves measured in compact tension specimens were also compared to those obtained in multi-specimen structural weld tests to examine the issue of transferability of R-curves.

Predictions of J - R curves were made using the Gurson-Tvergaard micromechanical model for the process of void growth that culminates in ductile crack growth [5]. A continuum model, it assumes the material acts as a homogenous, porous medium, such that the plastic flow potential is dependent on the hole volume fraction, f . The Gurson-Tvergaard model is implemented within a finite element framework (i.e., WARP3D) by discretizing the material ahead of the crack tip into uniform, fixed-sized cells, with each cell containing an initial void volume fraction, f_o . The cells lie in a single layer along the crack plane of height, D , where D is related to the mean spacing of large inclusions and comparable in size to the measured CTOD at the initiation of ductile tearing [5]. Void growth within the Gurson cells begins immediately upon loading (i.e., void nucleation is neglected). A critical void volume fraction, f_E , is used to assess coalescence. When $f \geq f_E$, the crack tip element is removed (and the crack tip advanced) computationally by reducing the remaining stresses in the element to zero [5].

As suggested by Kirk [2], a “bimetal” model of the weld/plate interface was used, in which the weld and plate are modeled as two distinct materials with no transition or HAZ. The crack front element size was selected from estimates of the weld metal fracture process zone obtained from test and metallographic data. The process zone size, D , was estimated to be about 0.008 inch. In the compact tension, bimetal analyses (with D fixed), f_o was varied to determine the best fit to the experimental C(T) J - R curves, load-CMOD data, and crack front shapes. For $D=0.008$ inch, it was determined after several iterations that the optimal initial void volume fraction for weld metal is 0.001, as shown in Fig. 1b. For comparison with the bimetal model, an “all weld metal” specimen, in which the entire specimen is modeled as one homogeneous material, was analyzed. As shown in Fig. 1b, J - R curve predictions made using the all weld metal model with fracture parameters found from the bimetal analysis diverge significantly from the experimental results. This result clearly illustrates the need to account for material property variations when dealing with welded materials.

Once calibrated with C(T) specimens, the model parameters ($D=0.008$ in and $f_o=0.001$) were used in a bimetal finite element analysis to predict the ductile fracture behavior of the more structurally representative CCP specimen geometry. Fig. 2a compares the crack growth profile at a given level of CMOD predicted

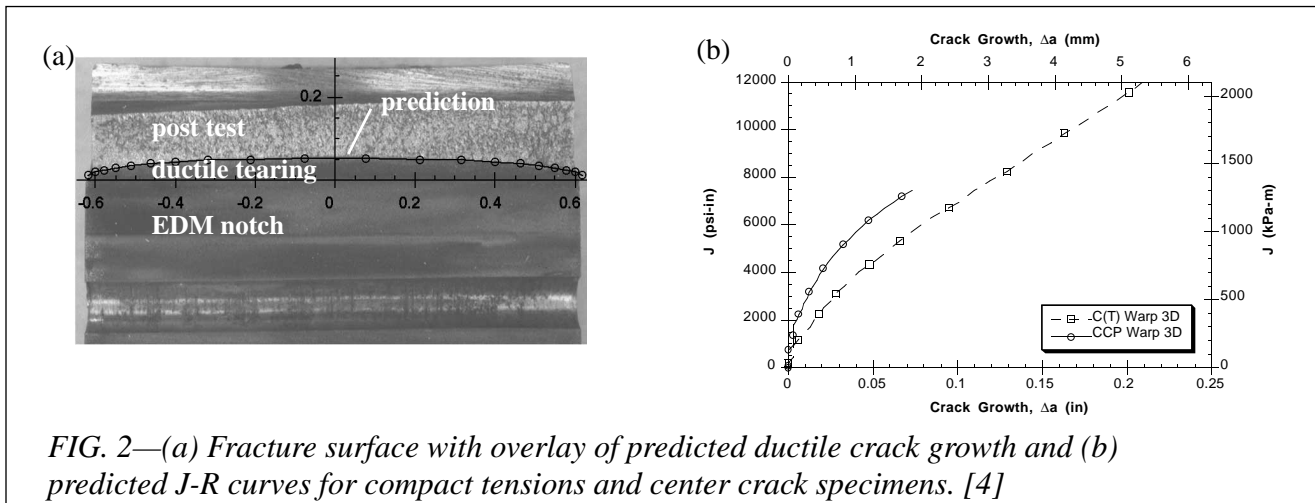


FIG. 2—(a) Fracture surface with overlay of predicted ductile crack growth and (b) predicted J - R curves for compact tensions and center crack specimens. [4]

by the analysis to that obtained experimentally. The predicted amount of crack growth is shown superimposed on the structural specimen fracture surface. The agreement is excellent. Comparison of the (predicted) C(T) and structural (CCP) J - R curves in Fig. 2b shows the specimen dependent toughness behavior consistent with previously demonstrated constraint effects [5].

Residual Stresses

The contribution of residual stresses to the driving force for fracture is well known. However, residual stresses may also affect apparent material toughness behavior by changing the constraint conditions under which fracture occurs. To investigate the constraint effects of residual stresses, Panontin and Hill [3] and Hill and Panontin [6] investigated computationally the micromechanics of cleavage fracture in the presence of a realistic residual stress field. The two crack geometries investigated are shown in Fig. 3: a girth-welded pipe representing a “structure” (Fig. 3a) and an SE(B) specimen removed from the structure (Fig. 3b). Homogeneous material properties were assumed to isolate the influence of residual stress on fracture. Material response was assumed to be elastic-plastic and to correspond to normalized A516-70, a high hardening, ferritic, pressure vessel steel with a uniaxial yield strength, σ_o , of 303 MPa (44 ksi).

A three-dimensional residual stress field representative in character of that developed in a two-sided multi-pass weld in a steel plate was considered. The crack plane distributions of residual stress in the pipe are plotted in Fig. 4. The residual stress field of Fig. 4 is generated within the finite element analysis by imposing an eigenstrain field. The label “eigenstrain” refers to the combination of all the non-elastic, incompatible strains set up during the welding cycle [3], which along with the geometry of the structure, completely defines the residual stress state. Here, an idealized eigenstrain distribution was assumed.

The Ritchie, Knott, and Rice, or RKR model for cleavage fracture was used to predict fracture initiation. The RKR model predicts fracture when the opening stress, σ_{yy} , ahead of the crack-tip exceeds a fracture stress, σ_f^* , over a critical distance, l^* [7]. The evolution of opening stress ahead of the crack-tip, due to applied loading alone or in combination with residual stress, was predicted using elastic-plastic, finite strain, finite element analysis. The RKR parameters were assumed to be $\sigma_f^* = 3.5\sigma_o$ and $l^* = 0.15$ mm (0.006 in), about 3 ferritic grain diameters in A516-70 [3].

The change in constraint conditions due to geometry and the influence of the residual stress field were quantified using J - Q theory. The theory uses an approximate two-parameter description of the crack-tip stress-strain fields developed from asymptotic analyses and finite element simulations performed by O’Dowd and Shih [8]. As a measure of how much σ_{ij} differs from the adopted small scale yielding (SSY) reference solution at the same applied J , the parameter Q has been shown to characterize the magnitude of the hydrostatic stress over the forward sector ahead of the crack-tip (i.e., $\theta < \pi/2$ and $1 < r/(J/\sigma_o) < 5$ to a good

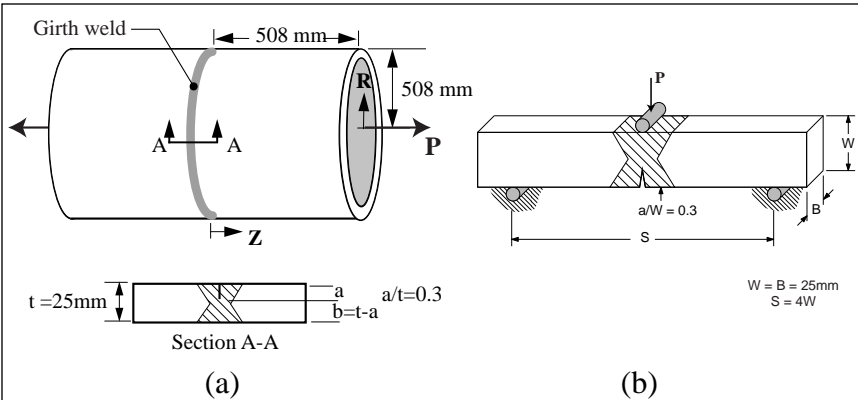


FIG. 3 -(a) pipe and (b) SE(B) specimens considered in residual stress study [9]

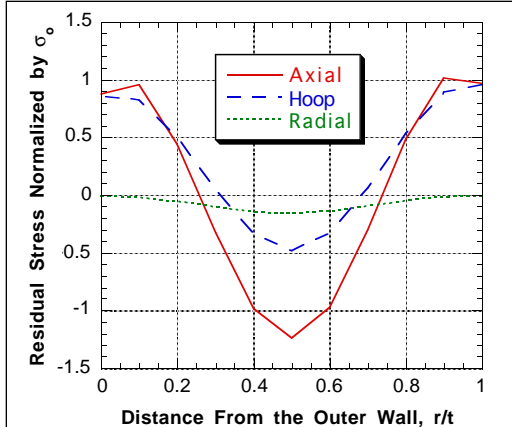


FIG. 4 - residual stress distribution in pipe specimen [9]

approximation. A negative Q -value denotes a loss in constraint, while a positive Q -value indicates that high constraint exists for a particular geometry and loading condition. In this study, Q was determined as

$$Q = [\sigma_{\theta\theta} - \sigma_{\theta\theta}|_{SSY}] / \sigma_o \text{ at } \theta = 0, r/(J/\sigma_o) = 4. \quad (1)$$

Fracture predictions using the superposition and RKR methods are reported in Table 1. At the load corresponding to RKR-predicted fracture, crack-tip opening stresses are nearly the same in each different geometry. As can be seen in Column 2 of Table 1, this occurs at markedly different values of J . For the two non-residual-stress, or “unwelded”, cases there is a large difference in RKR-predicted J at fracture, J_c . This demonstrates an anticipated constraint effect since the tension-loaded pipe is significantly less constrained than the SE(B) specimen. Constraint-loss increases crack-tip plasticity, so that additional loading is required to reach a critical crack-tip stress state. For the “welded” cases, the results show that cleavage fracture as predicted by the RKR model is severely affected by the residual stress field; the predicted J -integral for initiation in the pipe decreases by 63% and in the SE(B) geometry by 26%. The difference in the residual stress induced toughness change for each geometry (63% versus 26%) is thought to result from the relative absence of longitudinal welding residual stress in the SE(B) specimen, stresses acting in the hoop direction in the pipe which are released when the SE(B) is cut free.

The effect of geometry and residual stress on crack-tip constraint is also reflected in the J - Q trajectories for each specimen, shown in Fig. 5a. The final point (largest J) on each curve represents the point of predicted fracture initiation. The trajectory developed in the pipe geometry during loading without residual stresses demonstrates the immediate loss of constraint upon loading that is typical of a tension loaded, finite crack geometry. With residual stresses, however, the loss of constraint is delayed until later in the loading history. Near the predicted J -value for cleavage fracture initiation in the welded pipe, the Q -value for the welded pipe is still nearly 0.1 while that for the unwelded pipe is -0.4; this represents a large constraint increase created by the residual stresses. The increased constraint due to residual stress is also clearly mirrored in the plastic zone development at the crack tip, as shown in Fig. 5b. The residual stresses suppress crack tip plasticity and hence increase constraint.

Hill and Panontin [9] examined the accuracy of a superposition prediction of fracture by assuming that the RKR model correctly predicts fracture initiation and that the finite element prediction of J -integral correctly models the superposition of driving forces. A typical assessment would use J_c obtained from standard SE(B) specimen testing with an estimate of driving force to predict fracture (i.e., $J^{Total} = J_c$). The J_c value that would be measured in the unwelded SE(B) specimen in the study is $J_c = 17.0$ kN/m according to the RKR model (Table 1). Using this value of toughness to assess fracture in the unwelded pipe under-predicts the fracture load by 16%, relative to the RKR prediction of 21.3 MN. The prediction is in error because it assumes J -control of crack-tip stresses and ignores constraint-loss in the axially-loaded pipe relative to the SE(B). Using the same approach to predict fracture in the welded pipe, it was found that $J^{Total} = J_c$ at $P_c = 12.2$ MN. This load estimate is *non-conservative* by 24%, relative to the RKR prediction of $P_c = 9.83$ MN, because it ignores both the constraint-loss due to geometry and the constraint-addition caused

Geometry	J_c		Failure Load, P_c		
	RKR	RKR	Superposition with RKR J_c from:		
			SE(B)	Pipe	Welded SE(B)
SE(B)	17.0 kN/m	35.0 kN	--	--	--
Welded SE(B)	12.6 kN/m	11.7 kN	--	--	--
Pipe	36.7 kN/m	21.3 MN	17.9 MN	--	--
Welded Pipe	13.5 kN/m	9.83 MN	12.2 MN	19.9 MN	9.11 MN

Table 1: J -integral at fracture and fracture load predicted using the RKR and superposition models [9]

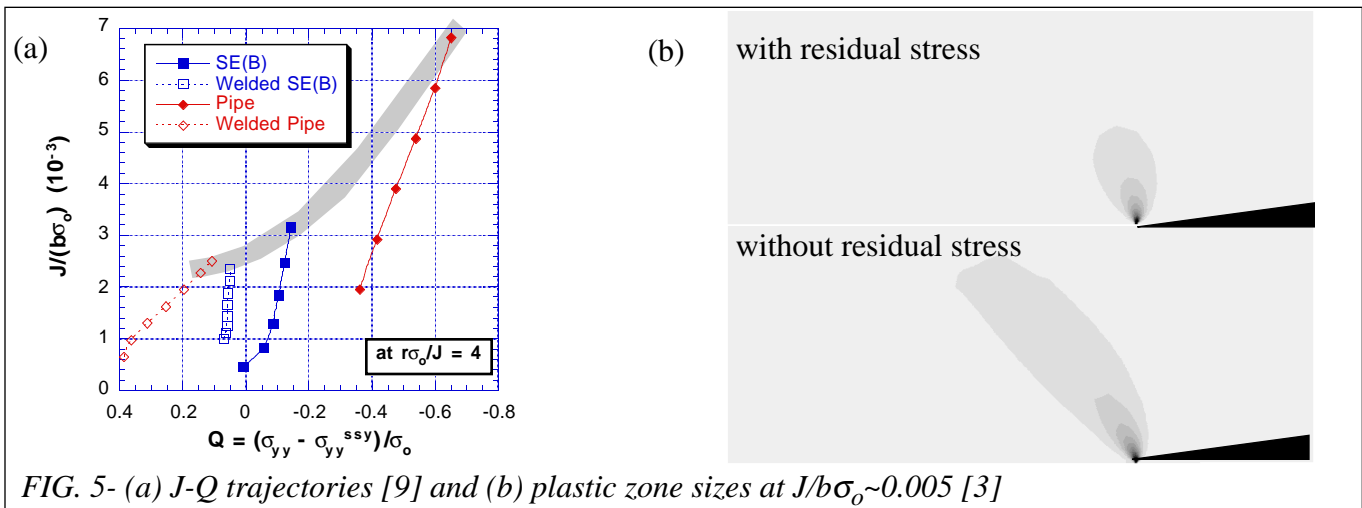


FIG. 5- (a) J - Q trajectories [9] and (b) plastic zone sizes at $J/b\sigma_0 \sim 0.005$ [3]

by residual stress. A toughness value might be obtained from the unwelded pipe to account for geometric constraint-loss in the pipe so that $J_c = 36.7$ kN/m. This leads to a prediction of fracture at $P_c = 19.9$ MN for the welded pipe, which is *non-conservative by 102%* because it ignores the constraint generated by residual stress.

Conclusions

Several studies were made to investigate the applicability of fracture assessment techniques to welded joints that contain fabrication defects, material property variations, and residual stresses. The results demonstrate the ability to predict ductile crack growth in stress-relieved defective structural welds using the computational cell methodology implemented in WARP3D when weld property differences are considered. Residual stresses are shown computationally to affect both the driving force for fracture and the constraint conditions at the crack tip. Results also show that superposition can account for the driving force but may produce serious errors if the constraint affect is ignored.

References

1. ASM Handbook, Vol. 6., "Welding, Brazing, and Soldering," ASM International, Metals Park, OH.
2. Kirk, M.T., "Predictions of Constraint Effects on Elastic-Plastic Fracture in Welded Structures," Ph.D. Thesis, Univ. of Illinois at Urbana Champaign, (1992).
3. Panontin, T. L. and Hill, M. R. "The Effect of Residual Stresses on Brittle and Ductile Fracture Initiation Predicted by Micromechanical Models," International Journal of Fracture v82 (1996) pp. 317-333.
4. Nishioka, O. and Panontin, T. L., "Ductile Crack Growth from Simulated Defects in Strength Overmatched Butt Welds," Fatigue and Fracture Mechanics: 29th Volume, ASTM STP 1321, West Conshohocken, PA, ASTM (to appear).
5. Ruggieri, C., Panontin, T. L., and Dodds, R. H., Jr. "Numerical Modeling of Ductile Crack Growth in 3-D Using Computational Cell Elements." International Journal of Fracture, v82 (1996) p. 67-95.
6. Hill, M. R. and Panontin, T. L., "Effect of Residual Stress on Brittle Fracture Testing," Fatigue and Fracture Mechanics: 29th Volume, ASTM STP 1321, West Conshohocken, PA, ASTM (to appear).
7. Ritchie, R. O., Server, W. L., and Wullarert, R. A., "Critical Fracture Stress and Fracture Strain Models for the Prediction of Lower and Upper Shelf Toughness in Nuclear Pressure Vessel Steels," Metallurgical Transactions 10A (1979) pp. 1557-1570.
8. O'Dowd, N. P. and Shih, C. F., "Family of Crack-Tip Fields Characterized by a Triaxiality Parameter: Part I-Structure of Fields," Journal of the Mechanics and Physics of Solids v39 (1991) pp. 989-1015.
9. Hill, M. R. and Panontin, T. L., "How Residual Stresses Affect Prediction of Brittle Fracture," in Fatigue, Fracture, and Residual Stresses, PVP series, New York, ASME (to appear),.